Physics Letters B 692 (2010) 232–239

Contents lists available at ScienceDirect

Physics Letters B

www.elsevier.com/locate/physletb

Measurement of $d\sigma/dy$ of Drell–Yan e^+e^- pairs in the Z mass region from $p\bar{p}$ collisions at $\sqrt{s} = 1.96$ TeV

CDF Collaboration

T. Aaltonen [z], J. Adelman [o], B. Álvarez González [m,24], S. Amerio [bc], D. Amidei [as], A. Anastassov [aw], A. Annovi [v], J. Antos [p,q], G. Apollinari [t], J. Appel [t], A. Apresyan [bk], T. Arisawa [bv], A. Artikov [r], J. Asaadi [bq], W. Ashmanskas [t], A. Attal [d], A. Aurisano [bq], F. Azfar [ba], W. Badgett [t], A. Barbaro-Galtieri [aj], V.E. Barnes [bk], B.A. Barnett [ab], P. Barria [bh], P. Bartos [p,q], G. Bauer [an], P.-H. Beauchemin [ao,ap,aq,ar], F. Bedeschi [bf], D. Beecher [al], S. Behari [ab], G. Bellettini [bg], J. Bellinger [bx], D. Benjamin [s], A. Beretvas [t], A. Bhatti [bm], M. Binkley [t,1], D. Bisello [bc], I. Bizjak [al,31], R.E. Blair [b], C. Blocker [h], B. Blumenfeld [ab], A. Bocci [s], A. Bodek [bl,*], V. Boisvert [bl], D. Bortoletto [bk], J. Boudreau [bj], A. Boveia [l], B. Brau [l,2], A. Bridgeman [aa], L. Brigliadori [g], C. Bromberg [at], E. Brubaker [o], J. Budagov [r], H.S. Budd [bl], S. Budd [aa], K. Burkett [t], G. Busetto [bc], P. Bussey [x], A. Buzatu [ao,ap,aq,ar], K.L. Byrum [b], S. Cabrera [s,26], C. Calancha [am], S. Camarda [d], M. Campanelli [al], M. Campbell [as], F. Canelli [o,t], A. Canepa [be], B. Carls [aa], D. Carlsmith [bx], R. Carosi [bf], S. Carrillo [u,15], S. Carron [t], B. Casal [m], M. Casarsa [t], A. Castro [g], P. Catastini [bh], D. Cauz [br], V. Cavaliere [bh], M. Cavalli-Sforza [d], A. Cerri [aj], L. Cerrito [al,18], S.H. Chang [ad,ae,af,ag,ah,ai], Y.C. Chen [a], M. Chertok [i], G. Chiarelli [bf], G. Chlachidze [t], F. Chlebana [t], K. Cho [ad,ae,af,ag,ah,ai], D. Chokheli [r], J.P. Chou [y], K. Chung [t,16], W.H. Chung [bx], Y.S. Chung [bl], T. Chwalek [ac], C.I. Ciobanu [bd], M.A. Ciocci [bh], A. Clark [w], D. Clark [h], G. Compostella [bb], M.E. Convery [t], J. Conway [i], M. Corbo [bd], M. Cordelli [v], C.A. Cox [i], D.J. Cox [i], F. Crescioli [bg], C. Cuenca Almenar [by], J. Cuevas [m,24], R. Culbertson [t], J.C. Cully [as], D. Dagenhart [t], N. d'Ascenzo [bd,23], M. Datta [t], T. Davies [x], P. de Barbaro [bl], S. De Cecco [bn], A. Deisher [aj], G. De Lorenzo [d], M. Dell'Orso [bg], C. Deluca [d], L. Demortier [bm], J. Deng [s,7], M. Deninno [f], M. d'Errico [bc], A. Di Canto [bg], B. Di Ruzza [bf], J.R. Dittmann [e], M. D'Onofrio [d], S. Donati [bg], P. Dong [t], T. Dorigo [bb], S. Dube [bp], K. Ebina [bv], A. Elagin [bq], R. Erbacher [i], D. Errede [aa], S. Errede [aa], N. Ershaidat [bd,30], R. Eusebi [bq], H.C. Fang [aj], S. Farrington [ba], W.T. Fedorko [o], R.G. Feild [by], M. Feindt [ac], J.P. Fernandez [am], C. Ferrazza [bi], R. Field [u], G. Flanagan [bk,20], R. Forrest [i], M.J. Frank [e], M. Franklin [y], J.C. Freeman [t], I. Furic [u], M. Gallinaro [bm], J. Galyardt [n], F. Garberson [l], J.E. Garcia [w], A.F. Garfinkel [bk], P. Garosi [bh], H. Gerberich [aa], D. Gerdes [as], A. Gessler [ac], S. Giagu [bo], V. Giakoumopoulou [c], P. Giannetti [bf], K. Gibson [bj], J.L. Gimmell [bl], C.M. Ginsburg [t], N. Giokaris [c], M. Giordani [bs], P. Giromini [v], M. Giunta [bf], G. Giurgiu [ab], V. Glagolev [r], D. Glenzinski [t], M. Gold [av], N. Goldschmidt [u], A. Golossanov [t], G. Gomez [m], G. Gomez-Ceballos [an], M. Goncharov [an], O. González [am], I. Gorelov [av], A.T. Goshaw [s], K. Goulianos [bm], A. Gresele [bc], S. Grinstein [d], C. Grosso-Pilcher [o], R.C. Group [t], U. Grundler [aa], J. Guimaraes da Costa [y], Z. Gunay-Unalan [at], C. Haber [aj], S.R. Hahn [t], E. Halkiadakis [bp], B.-Y. Han [bl], J.Y. Han [bl], F. Happacher [v], K. Hara [bt], D. Hare [bp], M. Hare [bu], R.F. Harr [bw], M. Hartz [bj], K. Hatakeyama [e], C. Hays [ba], M. Heck [ac], J. Heinrich [be], M. Herndon [bx], J. Heuser [ac], S. Hewamanage [e], D. Hidas [bp], C.S. Hill [l,4], D. Hirschbuehl [ac], A. Hocker [t], S. Hou [a], M. Houlden [ak], S.-C. Hsu [aj], R.E. Hughes [ax], M. Hurwitz [o], U. Husemann [by], M. Hussein [at], J. Huston [at], J. Incandela [l], G. Introzzi [bf], M. Iori [bo], A. Ivanov [i,17], E. James [t], D. Jang [n], B. Jayatilaka [s], E.J. Jeon [ad,ae,af,ag,ah,ai], M.K. Jha [f], S. Jindariani [t], W. Johnson [i], M. Jones [bk], K.K. Joo [ad,ae,af,ag,ah,ai], S.Y. Jun [n], J.E. Jung [ad,ae,af,ag,ah,ai], T.R. Junk [t], T. Kamon [bq], D. Kar [u], P.E. Karchin [bw], Y. Kato [az,14], R. Kephart [t], W. Ketchum [o], J. Keung [be], V. Khotilovich [bq], B. Kilminster [t], D.H. Kim [ad,ae,af,ag,ah,ai], H.S. Kim [ad,ae,af,ag,ah,ai], H.W. Kim [ad,ae,af,ag,ah,ai], J.E. Kim [ad,ae,af,ag,ah,ai], M.J. Kim [v], S.B. Kim [ad,ae,af,ag,ah,ai], S.H. Kim [bt], Y.K. Kim [o], N. Kimura [bv], L. Kirsch [h],

0370-2693/$ – see front matter
doi:10.1016/j.physletb.2010.06.043

S. Klimenko [u], K. Kondo [bv], D.J. Kong [ad,ae,af,ag,ah,ai], J. Konigsberg [u], A. Korytov [u], A.V. Kotwal [s], M. Kreps [ac], J. Kroll [be], D. Krop [o], N. Krumnack [e], M. Kruse [s], V. Krutelyov [l], T. Kuhr [ac], N.P. Kulkarni [bw], M. Kurata [bt], S. Kwang [o], A.T. Laasanen [bk], S. Lami [bf], S. Lammel [t], M. Lancaster [al], R.L. Lander [i], K. Lannon [ax,22], A. Lath [bp], G. Latino [bh], I. Lazzizzera [bc], T. LeCompte [b], E. Lee [bq], H.S. Lee [o], J.S. Lee [ad,ae,af,ag,ah,ai], S.W. Lee [bq,25], S. Leone [bf], J.D. Lewis [t], C.-J. Lin [aj], J. Linacre [ba], M. Lindgren [t], E. Lipeles [be], A. Lister [w], D.O. Litvintsev [t], C. Liu [bj], T. Liu [t], N.S. Lockyer [be], A. Loginov [by], L. Lovas [p,q], D. Lucchesi [bc], J. Lueck [ac], P. Lujan [aj], P. Lukens [t], G. Lungu [bm], J. Lys [aj], R. Lysak [p,q], D. MacQueen [ao,ap,aq,ar], R. Madrak [t], K. Maeshima [t], K. Makhoul [an], P. Maksimovic [ab], S. Malde [ba], S. Malik [al], G. Manca [ak,6], A. Manousakis-Katsikakis [c], F. Margaroli [bk], C. Marino [ac], C.P. Marino [aa], A. Martin [by], V. Martin [x,12], M. Martínez [d], R. Martínez-Ballarín [am], P. Mastrandrea [bn], M. Mathis [ab], M.E. Mattson [bw], P. Mazzanti [f], K.S. McFarland [bl], P. McIntyre [bq], R. McNulty [ak,11], A. Mehta [ak], P. Mehtala [z], A. Menzione [bf], C. Mesropian [bm], T. Miao [t], D. Mietlicki [as], N. Miladinovic [h], R. Miller [at], C. Mills [y], M. Milnik [ac], A. Mitra [a], G. Mitselmakher [u], H. Miyake [bt], S. Moed [y], N. Moggi [f], M.N. Mondragon [t,15], C.S. Moon [ad,ae,af,ag,ah,ai], R. Moore [t], M.J. Morello [bf], J. Morlock [ac], P. Movilla Fernandez [t], J. Mülmenstädt [aj], A. Mukherjee [t], Th. Muller [ac], P. Murat [t], M. Mussini [g], J. Nachtman [t,16], Y. Nagai [bt], J. Naganoma [bt], K. Nakamura [bt], I. Nakano [ay], A. Napier [bu], J. Nett [bx], C. Neu [be,28], M.S. Neubauer [aa], S. Neubauer [ac], J. Nielsen [aj,8], L. Nodulman [b], M. Norman [k], O. Norniella [aa], E. Nurse [al], L. Oakes [ba], S.H. Oh [s], Y.D. Oh [ad,ae,af,ag,ah,ai], I. Oksuzian [u], T. Okusawa [az], R. Orava [z], K. Osterberg [z], S. Pagan Griso [bc], C. Pagliarone [br], E. Palencia [t], V. Papadimitriou [t], A. Papaikonomou [ac], A.A. Paramanov [b], B. Parks [ax], S. Pashapour [ao,ap,aq,ar], J. Patrick [t], G. Pauletta [bs], M. Paulini [n], C. Paus [an], T. Peiffer [ac], D.E. Pellett [i], A. Penzo [br], T.J. Phillips [s], G. Piacentino [bf], E. Pianori [be], L. Pinera [u], K. Pitts [aa], C. Plager [j], L. Pondrom [bx], K. Potamianos [bk], O. Poukhov [r,1], F. Prokoshin [r,27], A. Pronko [t], F. Ptohos [t,10], E. Pueschel [n], G. Punzi [bg], J. Pursley [bx], J. Rademacker [ba,4], A. Rahaman [bj], V. Ramakrishnan [bx], N. Ranjan [bk], I. Redondo [am], P. Renton [ba], M. Renz [ac], M. Rescigno [bn], S. Richter [ac], F. Rimondi [g], L. Ristori [bf], A. Robson [x], T. Rodrigo [m], T. Rodriguez [be], E. Rogers [aa], S. Rolli [bu], R. Roser [t], M. Rossi [br], R. Rossin [l], P. Roy [ao,ap,aq,ar], A. Ruiz [m], J. Russ [n], V. Rusu [t], B. Rutherford [t], H. Saarikko [z], A. Safonov [bq], W.K. Sakumoto [bl], L. Santi [bs], L. Sartori [bf], K. Sato [bt], V. Saveliev [bd,23], A. Savoy-Navarro [bd], P. Schlabach [t], A. Schmidt [ac], E.E. Schmidt [t], M.A. Schmidt [o], M.P. Schmidt [by,1], M. Schmitt [aw], T. Schwarz [i], L. Scodellaro [m], A. Scribano [bh], F. Scuri [bf], A. Sedov [bk], S. Seidel [av], Y. Seiya [az], A. Semenov [r], L. Sexton-Kennedy [t], F. Sforza [bg], A. Sfyrla [aa], S.Z. Shalhout [bw], T. Shears [ak], P.F. Shepard [bj], M. Shimojima [bt,21], S. Shiraishi [o], M. Shochet [o], Y. Shon [bx], I. Shreyber [au], A. Simonenko [r], P. Sinervo [ao,ap,aq,ar], A. Sisakyan [r], A.J. Slaughter [t], J. Slaunwhite [ax], K. Sliwa [bu], J.R. Smith [i], F.D. Snider [t], R. Snihur [ao,ap,aq,ar], A. Soha [t], S. Somalwar [bp], V. Sorin [d], P. Squillacioti [bh], M. Stanitzki [by], R.St. Denis [x], B. Stelzer [ao,ap,aq,ar], O. Stelzer-Chilton [ao,ap,aq,ar], D. Stentz [aw], J. Strologas [av], G.L. Strycker [as], J.S. Suh [ad,ae,af,ag,ah,ai], A. Sukhanov [u], I. Suslov [r], A. Taffard [aa,7], R. Takashima [ay], Y. Takeuchi [bt], R. Tanaka [ay], J. Tang [o], M. Tecchio [as], P.K. Teng [a], J. Thom [t,9], J. Thome [n], G.A. Thompson [aa], E. Thomson [be], P. Tipton [by], P. Ttito-Guzmán [am], S. Tkaczyk [t], D. Toback [bq], S. Tokar [p,q], K. Tollefson [at], T. Tomura [bt], D. Tonelli [t], S. Torre [v], D. Torretta [t], P. Totaro [bs], M. Trovato [bi], S.-Y. Tsai [a], Y. Tu [be], N. Turini [bh], F. Ukegawa [bt], S. Uozumi [ad,ae,af,ag,ah,ai], N. van Remortel [z,3], A. Varganov [as], E. Vataga [bi], F. Vázquez [u,15], G. Velev [t], C. Vellidis [c], M. Vidal [am], I. Vila [m], R. Vilar [m], M. Vogel [av], I. Volobouev [aj,25], G. Volpi [bg], P. Wagner [be], R.G. Wagner [b], R.L. Wagner [t], W. Wagner [ac,29], J. Wagner-Kuhr [ac], T. Wakisaka [az], R. Wallny [j], S.M. Wang [a], A. Warburton [ao,ap,aq,ar], D. Waters [al], M. Weinberger [bq], J. Weinelt [ac], W.C. Wester III [t], B. Whitehouse [bu], D. Whiteson [be,7], A.B. Wicklund [b], E. Wicklund [t], S. Wilbur [o], G. Williams [ao,ap,aq,ar], H.H. Williams [be], P. Wilson [t], B.L. Winer [ax], P. Wittich [t,9], S. Wolbers [t], C. Wolfe [o], H. Wolfe [ax], T. Wright [as], X. Wu [w], F. Würthwein [k], A. Yagil [k], K. Yamamoto [az], J. Yamaoka [s], U.K. Yang [o,19], Y.C. Yang [ad,ae,af,ag,ah,ai], W.M. Yao [aj], G.P. Yeh [t], K. Yi [t,16], J. Yoh [t], K. Yorita [bv], T. Yoshida [az,13], G.B. Yu [s], I. Yu [ad,ae,af,ag,ah,ai], S.S. Yu [t], J.C. Yun [t], A. Zanetti [br], Y. Zeng [s], X. Zhang [aa], Y. Zheng [j,5], S. Zucchelli [g]

[a] *Institute of Physics, Academia Sinica, Taipei, Taiwan 11529, People's Republic of China*
[b] *Argonne National Laboratory, Argonne, IL 60439, USA*
[c] *University of Athens, 157 71 Athens, Greece*
[d] *Institut de Fisica d'Altes Energies, Universitat Autonoma de Barcelona, E-08193, Bellaterra (Barcelona), Spain*
[e] *Baylor University, Waco, Texas 76798, USA*
[f] *Istituto Nazionale di Fisica Nucleare Bologna, Italy*
[g] *University of Bologna, I-40127 Bologna, Italy*
[h] *Brandeis University, Waltham, MA 02254, USA*
[i] *University of California, Davis, Davis, CA 95616, USA*

[j] University of California, Los Angeles, Los Angeles, CA 90024, USA
[k] University of California, San Diego, La Jolla, CA 92093, USA
[l] University of California, Santa Barbara, Santa Barbara, CA 93106, USA
[m] Instituto de Fisica de Cantabria, CSIC-University of Cantabria, 39005 Santander, Spain
[n] Carnegie Mellon University, Pittsburgh, PA 15213, USA
[o] Enrico Fermi Institute, University of Chicago, Chicago, IL 60637, USA
[p] Comenius University, 842 48 Bratislava, Slovakia
[q] Institute of Experimental Physics, 040 01 Kosice, Slovakia
[r] Joint Institute for Nuclear Research, RU-141980 Dubna, Russia
[s] Duke University, Durham, NC 27708, USA
[t] Fermi National Accelerator Laboratory, Batavia, IL 60510, USA
[u] University of Florida, Gainesville, FL 32611, USA
[v] Laboratori Nazionali di Frascati, Istituto Nazionale di Fisica Nucleare, I-00044 Frascati, Italy
[w] University of Geneva, CH-1211 Geneva 4, Switzerland
[x] Glasgow University, Glasgow G12 8QQ, United Kingdom
[y] Harvard University, Cambridge, MA 02138, USA
[z] Division of High Energy Physics, Department of Physics, University of Helsinki and Helsinki Institute of Physics, FIN-00014, Helsinki, Finland
[aa] University of Illinois, Urbana, IL 61801, USA
[ab] The Johns Hopkins University, Baltimore, MD 21218, USA
[ac] Institut für Experimentelle Kernphysik, Karlsruhe Institute of Technology, D-76131 Karlsruhe, Germany
[ad] Center for High Energy Physics: Kyungpook National University, Daegu 702-701, Republic of Korea
[ae] Seoul National University, Seoul 151-742, Republic of Korea
[af] Sungkyunkwan University, Suwon 440-746, Republic of Korea
[ag] Korea Institute of Science and Technology Information, Daejeon 305-806, Republic of Korea
[ah] Chonnam National University, Gwangju 500-757, Republic of Korea
[ai] Chonbuk National University, Jeonju 561-756, Republic of Korea
[aj] Ernest Orlando Lawrence Berkeley National Laboratory, Berkeley, CA 94720, USA
[ak] University of Liverpool, Liverpool L69 7ZE, United Kingdom
[al] University College London, London WC1E 6BT, United Kingdom
[am] Centro de Investigaciones Energeticas Medioambientales y Tecnologicas, E-28040 Madrid, Spain
[an] Massachusetts Institute of Technology, Cambridge, MA 02139, USA
[ao] Institute of Particle Physics: McGill University, Montréal, Québec, Canada H3A 2T8
[ap] Simon Fraser University, Burnaby, British Columbia, Canada V5A 1S6
[aq] University of Toronto, Toronto, Ontario, Canada M5S 1A7
[ar] TRIUMF, Vancouver, British Columbia, Canada V6T 2A3
[as] University of Michigan, Ann Arbor, MI 48109, USA
[at] Michigan State University, East Lansing, MI 48824, USA
[au] Institution for Theoretical and Experimental Physics, ITEP, Moscow 117259, Russia
[av] University of New Mexico, Albuquerque, NM 87131, USA
[aw] Northwestern University, Evanston, IL 60208, USA
[ax] The Ohio State University, Columbus, OH 43210, USA
[ay] Okayama University, Okayama 700-8530, Japan
[az] Osaka City University, Osaka 588, Japan
[ba] University of Oxford, Oxford OX1 3RH, United Kingdom
[bb] Istituto Nazionale di Fisica Nucleare, Sezione di Padova-Trento, Italy
[bc] University of Padova, I-35131 Padova, Italy
[bd] LPNHE, Universite Pierre et Marie Curie/IN2P3-CNRS, UMR7585, Paris, F-75252, France
[be] University of Pennsylvania, Philadelphia, PA 19104, USA
[bf] Istituto Nazionale di Fisica Nucleare Pisa, Italy
[bg] University of Pisa, Italy
[bh] University of Siena, Italy
[bi] Scuola Normale Superiore, I-56127 Pisa, Italy
[bj] University of Pittsburgh, Pittsburgh, PA 15260, USA
[bk] Purdue University, West Lafayette, IN 47907, USA
[bl] University of Rochester, Rochester, NY 14627, USA
[bm] The Rockefeller University, New York, NY 10021, USA
[bn] Istituto Nazionale di Fisica Nucleare, Sezione di Roma 1, Italy
[bo] Sapienza Università di Roma, I-00185 Roma, Italy
[bp] Rutgers University, Piscataway, NJ 08855, USA
[bq] Texas A&M University, College Station, TX 77843, USA
[br] Istituto Nazionale di Fisica Nucleare Trieste/Udine, I-34100 Trieste, Italy
[bs] University of Trieste/Udine, I-33100 Udine, Italy
[bt] University of Tsukuba, Tsukuba, Ibaraki 305, Japan
[bu] Tufts University, Medford, MA 02155, USA
[bv] Waseda University, Tokyo 169, Japan
[bw] Wayne State University, Detroit, MI 48201, USA
[bx] University of Wisconsin, Madison, WI 53706, USA
[by] Yale University, New Haven, CT 06520, USA

ARTICLE INFO

Article history:
Received 28 March 2010
Received in revised form 21 May 2010
Accepted 22 June 2010
Available online 1 July 2010
Editor: H. Weerts

ABSTRACT

We report on a CDF measurement of the total cross section and rapidity distribution, $d\sigma/dy$, for $\gamma^*/Z \to e^+e^-$ events in the Z boson mass region ($66 < M_{ee} < 116$ GeV/c^2) produced in $p\bar{p}$ collisions at $\sqrt{s} = 1.96$ TeV with 2.1 fb^{-1} of integrated luminosity. The measured cross section of 257 ± 16 pb and $d\sigma/dy$ distribution are compared with Next-to-Leading-Order (NLO) and Next-to-Next-to-Leading-Order (NNLO) QCD theory predictions with CTEQ and MRST/MSTW parton distribution functions (PDFs).

Keywords:
Z boson
Rapidity $d\sigma/dy$
PDFs

There is good agreement between the experimental total cross section and $d\sigma/dy$ measurements with theoretical calculations with the most recent NNLO PDFs.

1. Introduction

Accurate predictions using perturbative quantum chromodynamics (QCD) are critical for understanding experimental results at hadron colliders. Such predictions depend on the accuracy of input parton distribution functions (PDFs), which at present cannot be calculated and are obtained from analysis of data from a broad range of processes. Precise knowledge of PDFs will be particularly important for analysis of data at the Large Hadron Collider (LHC) where new phenomena may be revealed via small deviations from Standard Model (SM) predictions. The Drell-Yan process [1], in which quark–antiquark annihilations form intermediate γ^* or Z (γ^*/Z) vector bosons decaying to lepton pairs, is particularly useful in providing information on PDFs at $Q^2 = M^2_{\ell\ell}$, where $M_{\ell\ell}$ is the invariant mass of the dilepton pair. In the leading order (LO) approximation, the momentum fractions x_1, x_2 carried by the initial state quarks in the proton and antiproton, respectively, are related to the rapidity y [2] of the γ^*/Z boson via the equation $x_{1,2} = (M_{\ell\ell}/\sqrt{s})e^{\pm y}$, where $\sqrt{s}$ is the center of mass energy. Dilepton pairs produced at large y originate from collisions in which one parton carries a large and the other a small momentum fraction x. A measurement of $d\sigma/dy$ at large y tests PDFs at high x, a region not well constrained by current results. Therefore, precise measurements of W and Z boson rapidity distributions at the Tevatron determine the size of higher order QCD terms and can be used to further refine current PDF models. Furthermore since the Z production cross section is predicted with an accuracy of $\approx 2\%$ [3], precise measurements of the rate of Z production at the Tevatron and the LHC can be used to determine the integrated luminosity [4] more precisely than the traditional method of using the total inelastic cross section. This has particular applicability to sub-processes initiated by a quark and an antiquark and can reduce the uncertainty in the determination of LHC and Tevatron cross sections.

The most recent Tevatron measurement of $d\sigma/dy$ for e^+e^- pairs in the Z boson mass region was performed by the D0 [5] experiment, using a data-set corresponding to 0.4 fb^{-1} of integrated luminosity. Here, we report on a new measurement of $d\sigma/dy$ at the Tevatron with an integrated luminosity of 2.1 fb^{-1}. The measured rapidity range extends to $|y| \sim 2.9$, close to the kinematic limit of $|y| = 3.0$ for Z boson production at $\sqrt{s} = 1.96$ TeV. The $d\sigma/dy$ distribution is compared to the predictions of perturbative QCD calculations in Next-to-Leading-Order (NLO) and Next-to-Next-to-Leading-Order (NNLO) with different PDF models.

2. Event selection and analysis method

The data sample corresponds to an integrated luminosity of 2.1 fb^{-1} collected by the CDF II Detector at Fermilab [6] during 2004–2007. CDF II uses a 1.4 T solenoidal magnetic spectrometer surrounded by projective-tower-geometry calorimeters and outer muon detectors. Charged particle directions and momenta are measured by an open-cell drift chamber (COT), a silicon vertex detector (SVX), and an intermediate silicon layer (ISL). The coverage of COT tracking in pseudorapidity is $|\eta| < 1.2$ [2]. Reconstructed tracks are used to determine the $p\bar{p}$ collision point along the beam line (z_{vertex}), which is required to be within $z = \pm 60$ cm of the detector. The energies and directions [2] of electrons, photons, and jets are measured by two separate calorimeters: central ($|\eta| < 1.1$) and plug ($1.1 < |\eta| < 3.6$). Each calorimeter has an electromagnetic (EM) compartment with a shower maximum detector followed by a hadronic (HAD) compartment. Three topologies of e^+e^- pairs are considered: two central electrons (CC), one central and one plug electron (CP), and two plug electrons (PP). The inclusion of PP events allows the measurement of Z bosons in the forward rapidity region which corresponds to high and low parton momentum fractions.

Data are collected using a three-level trigger system [6] and trigger paths with either one central electron or two electrons (central or plug) with transverse energy $E_T > 18$ GeV. Electron identification requirements [7] are imposed to select signal events and to suppress background. Both electron candidates are required to be isolated from any other calorimetric activity. The fraction of energy in the HAD calorimeter towers behind the EM shower is required to be small [7], as expected for an EM shower. Electron candidates with $E_T > 25$ GeV for CC and PP events, and $E_T > 20$ GeV for CP events, are selected in the central ($|\eta| < 1.1$), and plug ($1.2 < |\eta| < 2.8$) fiducial regions of the calorimeters. Central electron candidates must have a COT track that extrapolates to a shower cluster in the EM calorimeter and a track momentum consistent with the calorimeter measurement. Central and plug electron candidates are required to have EM-like transverse shower profiles using the shower maximum detectors. In order to reduce background we require that at least one of the plug electrons in PP events has a track reconstructed in the SVX that points

* Corresponding author.
E-mail address: bodek@pas.rochester.edu (A. Bodek).
[1] Deceased.
[2] Visitor from University of Massachusetts Amherst, Amherst, Massachusetts 01003, USA.
[3] Visitor from Universiteit Antwerpen, B-2610 Antwerp, Belgium.
[4] Visitor from University of Bristol, Bristol BS8 1TL, United Kingdom.
[5] Visitor from Chinese Academy of Sciences, Beijing 100864, China.
[6] Visitor from Istituto Nazionale di Fisica Nucleare, Sezione di Cagliari, 09042 Monserrato (Cagliari), Italy.
[7] Visitor from University of California Irvine, Irvine, CA 92697, USA.
[8] Visitor from University of California Santa Cruz, Santa Cruz, CA 95064, USA.
[9] Visitor from Cornell University, Ithaca, NY 14853, USA.
[10] Visitor from University of Cyprus, Nicosia CY-1678, Cyprus.
[11] Visitor from University College Dublin, Dublin 4, Ireland.
[12] Visitor from University of Edinburgh, Edinburgh EH9 3JZ, United Kingdom.
[13] Visitor from University of Fukui, Fukui City, Fukui Prefecture, 910-0017, Japan.
[14] Visitor from Kinki University, Higashi-Osaka City, 577-8502, Japan.
[15] Visitor from Universidad Iberoamericana, Mexico D.F., Mexico.
[16] Visitor from University of Iowa, Iowa City, IA 52242, USA.
[17] Visitor from Kansas State University, Manhattan, KS 66506, USA.
[18] Visitor from Queen Mary, University of London, London, E1 4NS, England.
[19] Visitor from University of Manchester, Manchester M13 9PL, England.
[20] Visitor from Muons, Inc., Batavia, IL 60510, USA.
[21] Visitor from Nagasaki Institute of Applied Science, Nagasaki, Japan.
[22] Visitor from University of Notre Dame, Notre Dame, IN 46556, USA.
[23] Visitor from Obninsk State University, Obninsk, Russia.
[24] Visitor from University de Oviedo, E-33007 Oviedo, Spain.
[25] Visitor from Texas Tech University, Lubbock, TX 79609, USA.
[26] Visitor from IFIC(CSIC-Universitat de Valencia), 56071 Valencia, Spain.
[27] Visitor from Universidad Tecnica Federico Santa Maria, 110v Valparaiso, Chile.
[28] Visitor from University of Virginia, Charlottesville, VA 22906, USA.
[29] Visitor from Bergische Universität Wuppertal, 42097 Wuppertal, Germany.
[30] Visitor from Yarmouk University, Irbid 211-63, Jordan.
[31] On leave from J. Stefan Institute, Ljubljana, Slovenia.

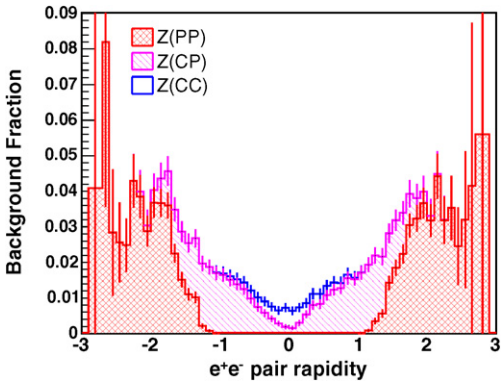

Fig. 1. The absolute fraction of QCD background events versus rapidity from the CC, CP, and PP e^+e^- topologies. The errors include the statistical and systematic uncertainties.

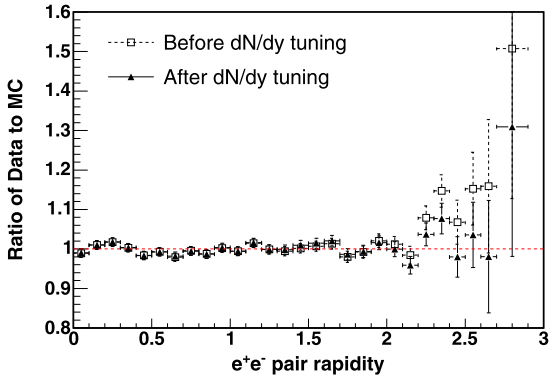

Fig. 2. The ratio of the rapidity distributions dN/dy of reconstructed e^+e^- pairs in data to the results from the simulation using PYTHIA, CTEQ5L LO PDFs and CDF W/Z tuning parameters [8]. The empty squires represent PYTHIA before modification of the rapidity distribution and the triangles represent PYTHIA after modification of the rapidity distribution.

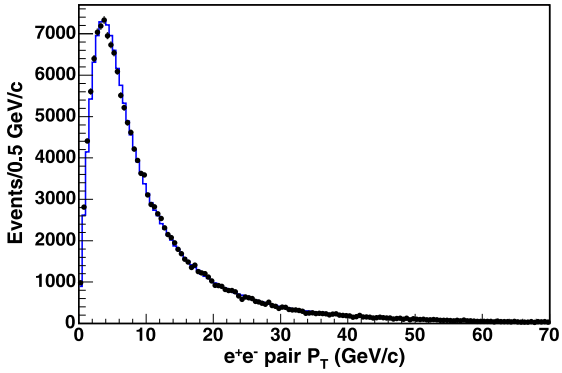

Fig. 3. The reconstructed transverse momentum distribution of e^+e^- pairs (after all event selection cuts) compared to the results from the simulation using PYTHIA, CTEQ5L LO PDFs and CDF W/Z tuning parameters [8]. The black points are CDF data and the blue solid line is the PYTHIA MC prediction. (For interpretation of the references to colour in this figure legend, the reader is referred to the web version of this Letter.)

to the EM cluster in the calorimeter. The efficiency of having at least one plug electron matched to an SVX track in PP events is about 85%. The selected number of CC, CP, and PP events with $66 < M_{ee} < 116$ GeV/c^2 is 50752, 86203, and 31415, respectively.

3. Backgrounds

The main backgrounds are QCD dijet and isolated photon plus jet events. Their fractional contributions in the CC, CP, and PP topologies are $0.24 \pm 0.03\%$ (stat $\oplus$ syst), $1.55 \pm 0.44\%$, and $3.40 \pm 0.75\%$, respectively. Their rapidity distributions are shown in Fig. 1. The shapes of the QCD backgrounds in rapidity are derived from the background samples, and their normalizations are derived from the events passing all selection cuts (the physics sample) as described below. The level and rapidity dependence of backgrounds from electroweak (WW, WZ, W + jets, and $Z \to \tau^+\tau^-$) and $t\bar{t}$ processes are derived from simulation; the overall level is $0.41 \pm 0.02\%$.

The dominant QCD dijet background is measured by statistically separating electrons from jets on the basis of E_T^{iso}, the transverse energy in a cone surrounding the center of the electromagnetic cluster in the calorimeter. QCD dijets have broad E_T^{iso} distributions while isolated electrons have E_T^{iso} distributions that are peaked at small E_T^{iso}. The background shape is obtained from a QCD enriched sample and the signal shape is obtained from Z boson enriched sample. For each e^+e^- pair topology, the E_T^{iso} distribution of the physics sample is fit to the signal and background shape to obtain the QCD dijet background fraction [7].

The fraction of the isolated photon plus jet events are about a third of the total CP and PP backgrounds and negligible in the CC topology. This background in each topology is determined by fitting its e^+e^- invariant mass distribution of the physics sample to a sum of the signal and backgrounds from QCD dijets, isolated photon plus jets, and electroweak processes [7]. The shapes of the isolated photon plus jet backgrounds are obtained from Monte Carlo simulations. The shapes of QCD dijet backgrounds are derived from the QCD enriched sample and their normalizations are fixed via the E_T^{iso} fits. These fits set the background fractions of the isolated photon plus jets.

4. Acceptance and efficiencies

The acceptance is defined as the ratio of the number of Monte Carlo (MC) simulation events that pass selection criteria in each y bin of the reconstructed final state e^+e^- pair (including resolution smearing) to the number of MC generated events in each true y bin of the generated γ^*/Z boson. The resolution in the measurement of the e^+e^- invariant mass is 2.2 GeV/c^2, and the resolution in the measurement of y is 0.015. The acceptance is modeled using the PYTHIA [8] generator combined with a GEANT [11] simulation of the CDF detector.

The PYTHIA generator begins with LO QCD $q + \bar{q} \to \gamma^*/Z \to e^+ + e^-$ interaction calculated with CTEQ5L [9] LO PDFs. It adds the higher order QCD and QED radiation effect via its parton shower machinery. There is an additional, ad-hoc, CDF tuning [8] added to accurately represent the Z boson transverse momentum distribution measured in data. The measured z_{vertex} distribution is included in the simulation (including its time dependence). To reconstruct the simulated events in the same way as data, the calorimetry energy scale, resolutions, and selection efficiencies used in the detector simulation are tuned using data. The selection efficiencies are functions of the pseudo rapidity of the electron, and the instantaneous luminosity [7]. The rapidity and time dependent efficiencies are extracted from the data and included in the Monte Carlo simulation. The acceptance depends on the modeling of the Z boson rapidity, the transverse momentum, and the angular distributions of the electron pairs, and these in turn depend on the event generator and the PDFs. We compare relevant kinematic distributions in the MC simulation to those observed in the data and correct the acceptance for the observed discrepancies.

While the generated rapidity spectrum is in good agreement with the data for $y < 2$, the data and simulation do not agree at

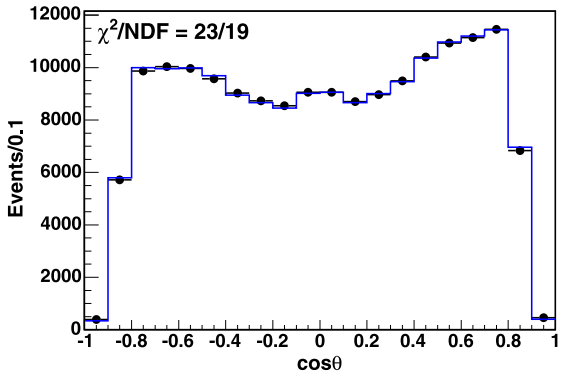

Fig. 4. The reconstructed polar angle distribution of e^+e^- pairs (after all event selection cuts) compared to the results from the simulation using PYTHIA, CTEQ5L LO PDFs and CDF W/Z tuning parameters [8]. The black points are CDF data and the blue solid line is the PYTHIA MC prediction. (For interpretation of the references to colour in this figure legend, the reader is referred to the web version of this Letter.)

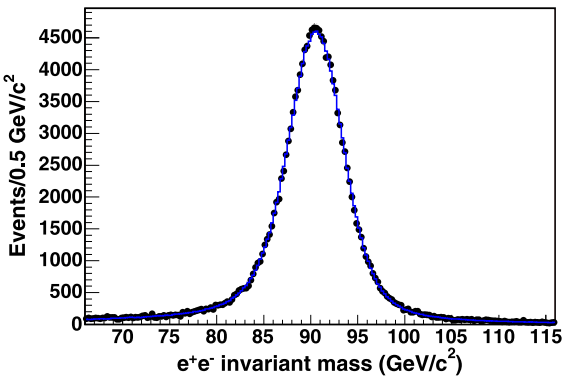

Fig. 5. The reconstructed mass distribution of e^+e^- pairs (after all event selection cuts) compared to the results from the simulation using PYTHIA, CTEQ5L LO PDFs and CDF W/Z tuning parameters [8]. The black points are CDF data and the blue solid line is the PYTHIA MC prediction. (For interpretation of the references to colour in this figure legend, the reader is referred to the web version of this Letter.)

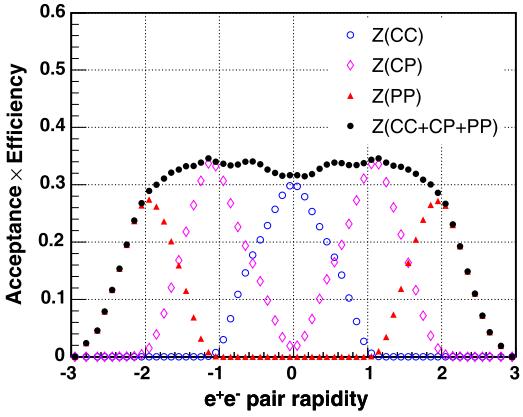

Fig. 6. The product of kinematic acceptance and event selection efficiency vs. the rapidity of the e^+e^- pair. The black points are the sum of all topologies.

larger values of y. To correct for this discrepancy, we modify the MC generated event spectrum (dN/dy) so that the final accepted MC spectrum matches the spectrum in data, as shown in Fig. 2. A comparison of the reconstructed transverse momentum spectra of the e^+e^- pairs in the data and the MC simulation reveals good agreement as shown in Fig. 3. Modifying the P_T spectrum in simulation to exactly follow the data leads to a negligible change in the calculated acceptance. There is a correlation between the P_T and y distributions of the final state boson, which leads to a reduction of the average P_T of events at large y. This correlation is well modeled by the simulation. Similarly, a study of the angular distribution in θ (where θ is the polar angle of the final state electron in the Collins-Soper frame [10]) in data shows good agreement with the simulation as illustrated in Fig. 4. The distributions of all variables such as the z_{vertex} distribution and electron kinematic variables (e.g. e^+e^- invariant mass, E_T, η) in data are in good agreement with the MC simulation. As an example, Fig. 5 compares the e^+e^- invariant mass distribution in the data with the MC simulation.

The acceptance (A) and efficiencies (ϵ) are determined as a function of boson rapidity. The contributions of each topology to the product $A \times \epsilon$ are shown in Fig. 6.

5. Differential and total cross sections

The differential cross section is given by

$$\frac{d\sigma(\gamma^*/Z)}{dy}(y) = \frac{N_{sig}(y) - N_{bkg}(y)}{c(y)\Delta y \epsilon_{zvtx} \Sigma_i [(A_i \times \epsilon_i(y)) \epsilon^i_{trig}(y) \mathcal{L}_i]}$$

where $N_{sig}(y) - N_{bkg}(y)$ is the number of events after subtracting background, $c(y)$ is a correction factor to convert the integrated $d\sigma/dy$ in a bin to $d\sigma/dy$ at the center of the bin, and Δy is the y bin size ($\Delta y = 0.1$ up to $y = 2.7$ and $\Delta y = 0.2$ for the last bin, $2.7 < y \leqslant 2.9$). The sum index i runs over the e^+e^- topologies (CC, CP, PP), $A_i \times \epsilon_i(y)$ is the combined acceptance and event selection efficiency, $\epsilon^i_{trig}(y)$ is the trigger efficiency, $\mathcal{L}_i$ is the total integrated luminosity for each topology, and ϵ_{zvtx} is the acceptance for the $p\bar{p}$ collision vertex to occur within $z = \pm 60$ cm of the center of the detector. The ϵ_{zvtx} in the data taken before June 2006 is $95.8 \pm 0.2\%$ and after that is $96.8 \pm 0.2\%$.

Systematic uncertainties in $d\sigma/dy$ originate from uncertainties in the estimates of the acceptance, backgrounds, electron identification efficiency, SVX tracking efficiency, and modeling of material in the detector. Uncertainties associated with correcting the acceptance for differences between kinematic distributions in data and simulation are found to be negligible.

The systematic uncertainty from each source is typically less than 0.5% except at the largest values of y. Detailed descriptions of all sources of the systematic uncertainty as a function of y are given in references [7,19]. The total systematic uncertainty is $\sim 1.0\%$ of $d\sigma/dy$ for $|y| < 2.5$, increasing to 10.0% at $|y| = 2.9$. The uncertainty on the integrated luminosity (lum.) is 6%. As shown in Fig. 7 and Table 1, the systematic error in $d\sigma/dy$ is about less than half of the statistical error for $|y| > 2$. Therefore, the experiment is still statistically limited. At the end of CDF run II (2011), with an integrated luminosity of 10 pb^{-1}, the statistical error can be reduced by more than a factor of 2 and become approximately equal to the total systematic error.

6. Results

Since the measured $d\sigma/dy$ values are symmetric about $y = 0$, the events for $y < 0$ are combined with the events for $y > 0$. The measured $d\sigma/dy$ values are shown versus $|y|$, with statistical and systematic uncertainties, in Fig. 7 and Table 1. The total cross section, derived from integrating $d\sigma/dy$ up to $|y| = 2.9$, is $\sigma = 256.6 \pm 0.7(\text{stat.}) \pm 2.0(\text{syst.}) \pm 15.4(\text{lum.})$ pb. These results are compared to QCD predictions at LO with CTEQ5L [9], at NLO [17] with MRST2001 (NLO) [14], MRST2004 (NLO) [15], CTEQ6.1M (NLO) [12], CTEQ6.6M (NLO) [13], and MSTW2008 (NLO) [3] PDFs, and at NNLO [18] with MRST2006E (NNLO) [16] and MSTW2008

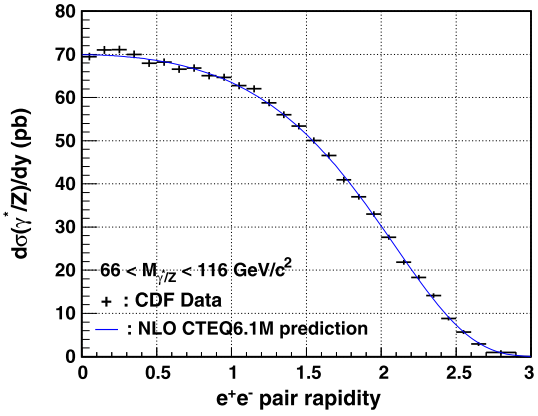

Fig. 7. The measured $d\sigma/dy$ for $p\bar{p} \to Z^0/\gamma^* \to e^+e^-$ over the entire rapidity range. The points are the measured cross section versus $|y|$ and the solid line is the theory prediction (scaled to the measured total cross section) for CTEQ6.1M(NLO) PDFs. The data points include the statistic and systematic uncertainties combined in quadrature.

Table 1
Differential cross sections for production of e^+e^- pairs in the mass range $66 < M_{ee} < 116$ GeV/c^2. The first and second uncertainties are statistical and systematical, respectively. The 6% luminosity uncertainty is not included. The quoted y values correspond to the center of the bin. The bin size is 0.1 up to $y = 2.7$ and 0.2 for the last bin.

y	$d\sigma/dy$ [pb]	y	$d\sigma/dy$ [pb]
0.05	$69.46 \pm 0.73 \pm 0.49$	1.55	$50.07 \pm 0.62 \pm 0.37$
0.15	$71.03 \pm 0.74 \pm 0.49$	1.65	$46.59 \pm 0.61 \pm 0.35$
0.25	$71.10 \pm 0.74 \pm 0.49$	1.75	$40.97 \pm 0.58 \pm 0.34$
0.35	$70.01 \pm 0.72 \pm 0.48$	1.85	$37.04 \pm 0.56 \pm 0.33$
0.45	$67.97 \pm 0.70 \pm 0.47$	1.95	$33.02 \pm 0.55 \pm 0.31$
0.55	$68.22 \pm 0.70 \pm 0.47$	2.05	$27.65 \pm 0.52 \pm 0.25$
0.65	$66.58 \pm 0.69 \pm 0.47$	2.15	$21.84 \pm 0.49 \pm 0.23$
0.75	$66.81 \pm 0.70 \pm 0.48$	2.25	$18.35 \pm 0.50 \pm 0.20$
0.85	$65.05 \pm 0.69 \pm 0.49$	2.35	$14.13 \pm 0.49 \pm 0.17$
0.95	$64.70 \pm 0.69 \pm 0.50$	2.45	$8.80 \pm 0.45 \pm 0.10$
1.05	$62.74 \pm 0.67 \pm 0.50$	2.55	$5.68 \pm 0.44 \pm 0.09$
1.15	$62.02 \pm 0.66 \pm 0.49$	2.65	$2.93 \pm 0.41 \pm 0.15$
1.25	$58.80 \pm 0.65 \pm 0.48$	2.80	$0.87 \pm 0.22 \pm 0.11$
1.35	$56.02 \pm 0.65 \pm 0.43$	2.95	–
1.45	$53.37 \pm 0.63 \pm 0.40$		

Table 2
A comparison of the measured total cross section for the production of e^+e^- pairs in the mass range $66 < M_{ee} < 116$ GeV/c^2 to theory calculations.

Model	Total cross section [pb]
CTEQ5L(LO)	183.3
MRST2001E(NLO)	$241.0^{+2.8}_{-3.4}$
MRST2004(NLO)	241.2
MSTW2008E(NLO)	$242.6^{+4.6}_{-5.5}$
CTEQ6.1M(NLO)	$236.1^{+9.3}_{-9.2}$
CTEQ6.6M(NLO)	$238.7^{+7.1}_{-7.0}$
MRST2006E(NNLO)	$251.6^{+2.8}_{-3.1}$
MSTW2008E(NNLO)	$248.7^{+5.1}_{-4.0}$
Data	$256.6 \pm 0.7 \pm 2.0 \pm 15.4$

(NNLO) [3] PDFs. The measured total cross section is consistent with both NLO and NNLO calculations as shown in Table 2.

In comparing the shape of the measured $d\sigma/dy$ to theory, the latter distributions are normalized to the measured total cross section of 256.6 pb. The ratios of the measured $d\sigma/dy$ to the QCD calculations at LO, NLO and NNLO with the above mentioned PDFs are shown in Figs. 8, 9, and 10. The shaded bands in the figures correspond to the uncertainties associated to the MSTW2008E

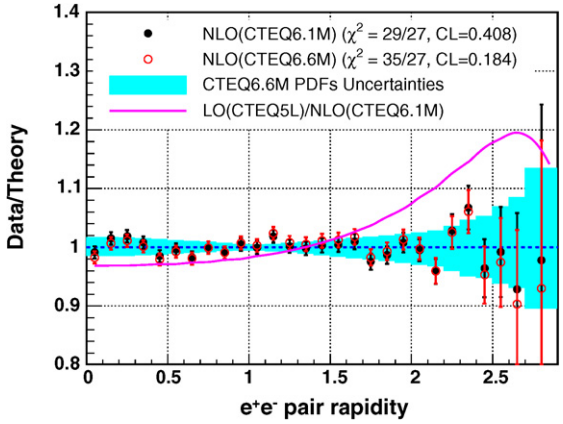

Fig. 8. The ratio of the experimental distribution of $d\sigma/dy$ (statistical and systematic uncertainties combined) to the NLO theoretical predictions with CTEQ PDFs (CTEQ6.1M and CTEQ6.6M). The shaded bands corresponds to the CTEQ6.6M PDFs 90% C.L. uncertainties. The χ^2 test includes the data statistical and systematical uncertainties. The solid line is the ratio of LO(CTEQ5L) to NLO(CTEQ6.1M) predictions. All theoretical distributions are normalized to the measured total cross section of 256.6 pb.

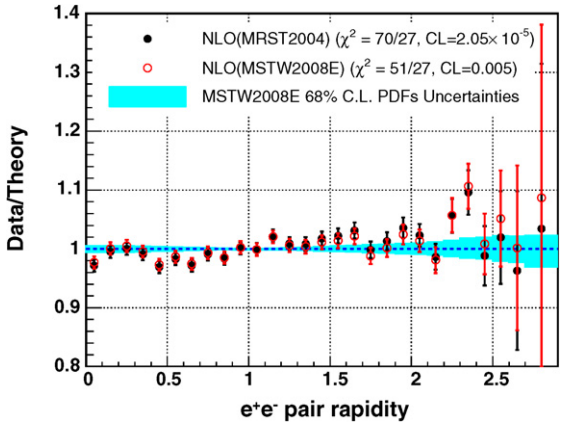

Fig. 9. The ratio of the experimental distribution of $d\sigma/dy$ (statistical and systematic uncertainties combined) to the NLO theoretical predictions with MRST2004 and MSTW2008E NLO PDFs. The shaded bands corresponds to the MSTW2008E PDFs 68% C.L. uncertainties. The χ^2 test includes the data statistical and systematical uncertainties. All theoretical distributions are normalized to the measured total cross section of 256.6 pb.

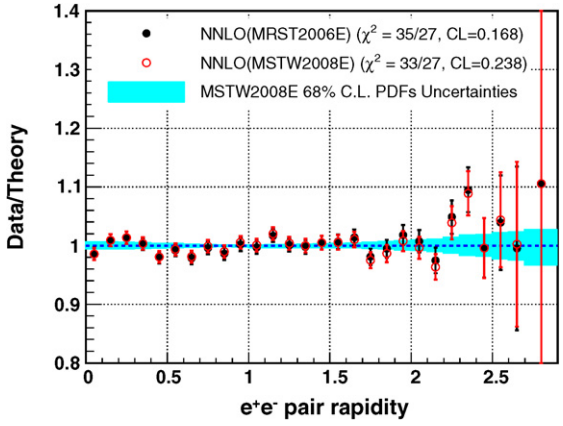

Fig. 10. The ratio of the experimental distribution of $d\sigma/dy$ (statistical and systematic uncertainties combined) to the NNLO theoretical predictions with MRST2006E and MSTW2008E NNLO PDFs. The shaded bands corresponds to the MSTW2008E PDFs 68% C.L. uncertainties. The χ^2 test includes the data statistical and systematical uncertainties. All theoretical distributions are normalized to the measured total cross section of 256.6 pb.

Table 3
A comparison of the shape of the measured $d\sigma/dy$ distribution to theoretical predictions with several choices of PDFs. The theoretical distributions are normalized to the measured total cross section of 256.6 pb. The χ^2 for 27 degrees of freedom includes statistical and systematic uncertainties.

Model	χ^2/DOF	CL
CTEQ5L(LO)	242/27	–
MRST2001E(NLO)	76/27	2.908×10^{-6}
MRST2004(NLO)	70/27	2.049×10^{-5}
MSTW2008E(NLO)	51/27	0.005
CTEQ6.1M(NLO)	29/27	0.408
CTEQ6.6M(NLO)	35/27	0.184
MRST2006E(NNLO)	35/27	0.168
MSTW2008E(NNLO)	33/27	0.238

(NLO and NNLO) PDFs, which are given with 68% C.L. errors and to the those associated to the other sets of PDFs, given with 90% C.L. errors. A χ^2 comparison (including statistical and systematic uncertainties) is shown in Table 3. Better agreement is obtained for the MSTW (2008) PDF at NNLO compared to NLO. The NLO CTEQ6.1M, CTEQ6.6M, the NNLO MRST2006 and MSTW2008 PDFs all describe the data well. The older NLO MRST (2004) set provides a poorer description of the data and, as expected, so does the LO PDF, CTEQ5L. The MSTW (2008) PDF used a preliminary version of the data presented in this Letter in their fit. The correlations [7,19] between the uncertainties in different y bins are included in the χ^2 comparison.

In summary, the high-statistics measurements of the total cross section and $d\sigma/dy$ in the γ^*/Z production with the Z mass region are found to agree with theoretical calculations that use recent NLO and NNLO PDFs. The total cross section is measured to be $\sigma = 256.6 \pm 2.1(\text{stat} \oplus \text{syst}) \pm 15.4(\text{lum.})$ pb. The traditional method of using the total inelastic cross section gives a large error which is not reducible. This precise measurement of the total cross section can be used to set the integrated luminosity more precisely at the Tevatron and the LHC once the PDFs error goes down. (The total error for the measurement is less than 1% excluding the luminosity error, 6%, while the PDFs error is up to 4%.)

Acknowledgements

We thank the Fermilab staff and the technical staffs of the participating institutions for their vital contributions. This work was supported by the US Department of Energy and National Science Foundation; the Italian Istituto Nazionale di Fisica Nucleare; the Ministry of Education, Culture, Sports, Science and Technology of Japan; the Natural Sciences and Engineering Research Council of Canada; the National Science Council of the Republic of China; the Swiss National Science Foundation; the A.P. Sloan Foundation; the Bundesministerium für Bildung und Forschung, Germany; the World Class University Program, the National Research Foundation of Korea; the Science and Technology Facilities Council and the Royal Society, UK; the Institut National de Physique Nucleaire et Physique des Particules/CNRS; the Russian Foundation for Basic Research; the Ministerio de Ciencia e Innovación, and Programa Consolider-Ingenio 2010, Spain; the Slovak R&D Agency; and the Academy of Finland. We also thank Robert Thorne for valuable discussions.

References

[1] S.D. Drell, T.-M. Yan, Phys. Rev. Lett. 25 (1970) 316.
[2] CDF coordinates are (θ,ϕ,z), where θ is the polar angle relative to the proton beam (the $+z$ axis), and ϕ the azimuth. The pseudorapidity is $\eta = -\ln\tan(\theta/2)$. For an $e^+ + e^-$ pair $P_T = P\sin\theta$, $E_T = E\sin\theta$, and $y = \frac{1}{2}\ln\frac{E+P_z}{E-P_z}$, where P and P_z are the magnitude and z component of the momentum, and E is the energy of the $e^+ + e^-$ pair.
[3] A.D. Martin, W.J. Stirling, R.S. Thorne, G. Watt, Eur. Phys. J. C 63 (2009) 189. A preliminary version of these results has been used in the determination of these PDFs.
[4] M. Dittmar, F. Pauss, D. Zurcher, Phys. Rev. D 56 (1997) 7284;
V.A. Khoze, A.D. Martin, R. Orava, M.G. Ryskin, Eur. Phys. J. C 19 (2001) 313.
[5] V.M. Abazov, et al., D0 Collaboration, Phys. Rev. D 76 (2007) 012003.
[6] The CDF II Detector Technical Design Report, Fermilab-Pub-96/390-E;
D. Amidei, et al., Nucl. Instrum. Methods Phys. Res. A 350 (1994) 73;
F. Abe, et al., Phys. Rev. D 52 (1995) 4784;
P. Azzi, et al., Nucl. Instrum. Methods Phys. Res. A 360 (1995) 137;
D. Acosta, et al., CDF Collaboration, Phys. Rev. D 71 (2005) 032001.
[7] Han Jiyeon, Ph.D. thesis, University of Rochester, FERMILAB-THESIS-2008-65.
[8] T. Sjøstrand, et al., JHEP 0605 (2006) 026. We use the default (MSEL = 11) LO matrix element ($Z + 0$ jet) with CTEQ5L PDFs and electroweak coupling $\sin^2\theta_W = 0.232$. The parton showering produces the boson P_T. The CDF EWK/TOP standard W/Z P_T tuning parameters are: MSTP(91) = 1, PARP(91) = 2.10, PARP(93) = 15 for the low P_T Gaussian smearing, with PART(62) = 1.25 and PARP(62) = 0.2 for the P_T evolution in 7–25 GeV region. The underlying event is included as Tune A.
[9] H.L. Lai, et al., Eur. Phys. J. C 12 (2000) 375.
[10] J.C. Collins, D.E. Soper, Phys. Rev. D 16 (1977) 2219.
[11] GEANT: CERN Program Library Long Writeup W5013, 1993.
[12] J. Pumplin, D.R. Stump, J. Huston, H.L. Lai, P. Nadolsky, W.K. Tung, JHEP 0207 (2002) 012;
J. Pumplin, D.R. Stump, J. Huston, H.L. Lai, W.K. Tung, S. Kuhlmann, J.F. Owens, JHEP 0310 (2003) 046.
[13] P. Nadolsky, H.L. Lai, Q.H. Cao, J. Huston, J. Pumplin, D. Stump, W.K. Tung, C.P. Yuan, Phys. Rev. D 78 (2008) 013004.
[14] A.D. Martin, R.G. Roberts, W.J. Stirling, R.S. Thorne, Eur. Phys. J. C 28 (2003) 455.
[15] A.D. Martin, R.G. Roberts, W.J. Stirling, R.S. Thorne, Phys. Lett. B 604 (2004) 61.
[16] A.D. Martin, W.J. Stirling, R.S. Thorne, G. Watt, Phys. Lett. B 652 (2007) 292.
[17] P.J. Sutton, A.D. Martin, R.G. Roberts, W.J. Stirling, Phys. Rev. D 45 (1992) 2349.
[18] P.J. Rijken, W.L. van Neerven, Phys. Rev. D 51 (1995) 44;
$\overline{MS}$ NNLO for $d^2\sigma/dy\,dM$: C. Anastasiou, L. Dixon, K. Melnikov, F. Petriello, Phys. Rev. D 69 (2004) 094008.
[19] CERN ROOT C++ code for $d\sigma/dy$ and statistical and systematic uncertainty contributions from each source including correlations is available at http://www-cdf.fnal.gov/physics/ewk/2009/dszdy.